Int. J. Adv. Appl. Math. and Mech. 10(3) (2023) 1 – 20 (ISSN: 2347-2529)

Journal homepage: www.ijaamm.com

International Journal of Advances in Applied Mathematics and Mechanics

Pressure Performance Equation of a Horizontal Well in a Completely Bounded Isotropic Reservoir

Research Article

Bakary L. Marong[a, *], **Phineas Roy Kiogora**[b], **Kennedy Otieno Awuor**[c]

[a] *Department of Mathematics, Pan African University, Institute for Basic Sciences Technology and Innovation, Gachoro, 00200, Nairobi, Kenya*

[b] *Mathematics Department, Jomo Kenyatta University of Agriculture and Technology, Gachoro, 00200, Nairobi, Kenya*

[c] *Mathematics and Actuarial Science Department, Kenyatta University, Kenyatta Road, 00200, Nairobi, Kenya*

Received 11 November 2022; accepted (in revised version) 07 January 2023

Abstract: A well test or well testing is considered as an elaborate plan of activity by an engineer to acquire, analyze and understand data about the properties of hydrocarbons which are trap below the surface of the earth in a reservoir and use the data to understand the reservoir itself. We solved the mathematical models of the flow regimes, the dimensionalized flow regimes were plot on a log-log axis, and the results were implemented in MATLAB. Dimensionless reservoir length, x_{eD} is inversely proportional to both dimensionless pressure, P_D and dimensionless pressure derivative, $P_{D'}$ when all the boundaries have been felt by the flow. The findings of the study are applicable in appraising fewer number of wells with higher production, Civil engineering, Mining, Geology, Geophysics, and Petrophysics.

MSC: 76S05 • 76T30

Keywords: Dimensionless pressure • Dimensionless pressure derivatives • Horizontal well

1. Introduction

A well test or well testing can be considered as an elaborate plan of activities by an engineer to acquire, analyse and understand data about the properties of hydrocarbons which are trapped below the surface of the earth in a reservoir and also use the data to understand the reservoir itself. This data provides information about the ability of a reservoir to produce hydrocarbons. [1]observed that this whole process intents to obtain: reservoir pressure, completion efficiency, distance to the boundaries, formation damage, vertical layering, aerial extent, drawdown pressure, fluid properties, permeability, flow rates, formation heterogeneity, production capacity, productivity index, and other details relevant to the test. If this data can be obtained and analysed, well test analysis is the process where pressure transient analysis is conducted either to confirm production ability or to enhance performance. [2]noted that well test analysis to be considered as a wide area of reservoir engineering which involves the comprehension of the reservoir characteristics including the rock properties by applying different techniques. [3]noted that, this process provides information of both the well and the reservoir which contain the hydrocarbon in which well test analysis will involve the best model to interpret the pressure response. He noted that for an exploration well, the initial pressure, reservoir properties, nature and the rate of production would be the main objectives of a well test. For an appraisal

* Corresponding author.

E-mail address(es): marongbakary1993@email.com (Bakary L. Marong), prkiogora@jkuat.ac.ke (Phineas Roy Kiogora), awuor.kennedy@ku.ac.ke (Kennedy Otieno Awuor).

well, one would need to conduct a well test to refine a reservoir description while for a development well, the well test would be used to adjust the reservoir description as well as establish pressure communication between wells.
The three main types of well testing methods that has been employed through several years are drawdown test, buildup test and Interference test.

Drawdown test

In a drawdown test, a well which is shut-in is opened to flow. The main objectives of the drawdown test are to: obtain average permeability of the drainage area, estimate skin, obtain a pore of the reservoir and detect reservoir heterogeneity.

Buildup test

A producing well is shut down and a bottom hole pressure (BHP) is measured in a buildup test. To offer information on permeability and skin thickness for reservoir characterization. The results of a buildup test can also be used to monitor a reservoir, specifically reservoir pressure data.

Interference test

At least two wells are employed in interference testing, the wells can be in the same layer or different layer, and they can also be both horizontal or vertical wells or of different wells. The active well is put on production while the observational well is use to monitor the pressure and production rate and there is a pressure communication between the two wells in a reservoir. The observation well pressure response enables us to determine multiple well tests. We should observe when building an interference test, it will be preferable to build an active well rather than an injection well.

2. Statement of the Problem

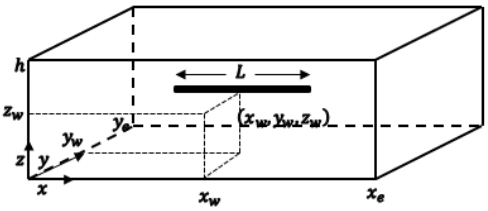

Physical Model of a Horizontal Oil Well in a Rectangular Drainage Volume

Fig. 1

This physical model considers a horizontal well in a rectangular drainage volume of length x_e in the x-direction, width y_e in the y-direction and thickness h in the z-direction, since the reservoir is assumed to be homogeneous and isotropic, then the formation permeability is equal to the axial permeability's. A horizontal oil well of length L which is assumed to be parallel to the x-axis is considered. The oil well is centrally located at (x_w, y_w, z_w) stretching a length of $\frac{L}{2}$ from x_w in both directions along x and the source geometry used as given by[4]
The isotropic homogeneous reservoir with sealed boundaries where the well was a line source and eccentric was neglected by many researchers, hence this study has investigated the well test analysis of horizontal well in a completely bounded reservoir where the four flow regimes were solved by considering a line source model. It is also clear that horizontal well analysis is more difficult than vertical well analysis, this is because assessing the flow into a horizontal well requires three dimensions as opposed to a single flow for vertical wells. Horizontal wells are more expensive to drill compared to vertical wells.

3. Literature Review

[5] investigated that working equations which allow us to process field data when the flow rate at the active well is a function of time. The shut-in period is also considered. A new method of field data processing, where all pressure drops are utilized was also studied. They developed working equations which will allow them to process field data when the flow rate at the active well is a quadratic function with respect to time. A type-curve matching technique is used. The graph of pressure drop against time was plotted where both the minimum and maximum pressure drop

was obtained.
[6] studied the characterization of volatile oil reservoirs using well test analysis. Typical well test behaviors were counterfeit for varied production rates, fluid formation, and relative permeability curves with bottom hole pressures above and below the bubble point pressure using a one-dimensional single well structural reservoir model. During a drawdown, as the bottom hole pressure falls below the bubble point pressure, a high gas saturation zone with two-phase (oil and gas) flow forms near the wellbore, whereas single phase (oil) flow with the original gas saturation persists away from the wellbore.The modified Peng-Robinson equation of state (EOS) with three parameters was used for modeling PVT properties of reservoir fluids. Regression was performed on molecular weight (MW) of heavy components, critical pressure (P_c) and critical temperature (T_c) of the pseudo-components and binary interaction coefficients between light and heavy components

[7] compared the pressure behavior between a horizontal well and a vertical well subject to edge water drive. They used source and Green's function to evaluate the performance of vertical and horizontal wells. The results obtained indicated that the rate of decline for vertical wells was sharper and more sensitive compared to horizontal wells in the pressure derivative curves. They concluded that,would indicate a shorter period for vertical wells compared to horizontal wells.

[8] discussed the presence of more than one active well in interference tests using synthetic data. At first analysis of data will be presented where pressure of other wells are ignored. Errors will be discussed thoroughly.Finally, data from a geothermal reservoir will be used to present interference test design and analysis that includes the effects of other flowing wells using superposition in time and space. The proposed multi-well analytical simulation model using the concept of mathematical superposition in time and space of the aforementioned exponential integral solution. Two wells that will be used in a new power plant are to be tested by flowing one well and observing the pressure change in the other well.The locations of the wells and finite conductivity faults are given. The model simulated an interference test conducted in a double porosity reservoir with well bore storage and effects.

[9] investigated the impact of well interference on in-situ stresses, drainage area and examine the pressure response in hydraulically fractured shale reservoirs. This study was done using iterative numerical methods and applied on hydraulically fractured shale reservoirs. The results obtained suggested that the drainage distance as measured from the well centre is restricted to the location of the well and thus the effect on the external reservoir was almost negligible.

[10] investigated the performance of a horizontal well between two parallel sealing faults.They looked at how different parameters affected the dimensionless pressure and pressure derivative. Finally discovered that increased in perforation length reduces the production potential of the horizontal well. Analytical solution of source and Green's function method was employed. It was obtained that high vertical permeability shortens the effect of the early radial flow.

[11] established a well test model for fractured horizontal wells in tight gas reservoirs considering complex fracture networks. Well test log-log type curves of fractured horizontal well were obtained. They analyzed the characteristics of well test curves and their influencing factors and compared them with the well test curves from the conventional single fracture model. They solved the model using finite element method of triangular unit and line unit. The calculation results of the proposed model are compared with that of the commercial well testing software Saphir. Given the same stimulated area, the well test curves of horizontal well with a stimulated area length of 245m, 173m, and 122m and the width-to-length ratio of 0.1, 0.2, and 0.4 were calculated.

[12] investigated the reservoir and well settings that will allow the reservoir's steady state activity to continue indefinitely. They look at parameters using a mathematical model and calculate the findings in a dimensionless format. To analyze pressure responses in the reservoir, they use source and Green's function. The result show a progressive rise in P_D at early time at $t_D \geq \frac{L_D}{5}$, this is a characteristics signature of an infinite acting flow period.

[13] devised a horizontal well test, but only considered an infinite-acting well. The advancements in well test analysis have been discussed. They analyze a completely constrained reservoir and investigate the impact of all reservoir and well parameters in all three dimensions on the horizontal well's pressure response. Mathematical procedure leading to this method of analysis is based on relevant source and Green's function. Straight line relationship exists between two plotted parameters on a linear paper. From the plot reservoir pressure, near wellbore permeability, reservoir capacity fluid mobility and transmissibility were obtained.
[14]Carbonate reservoirs usually have strong anisotropy. Oil and gas recovery from fractured reservoirs is highly challenging due to complicated mechanism involved in production from these reservoirs. A multizone triple-porosity model was established and solved by using the point source function, Green's function, and coupling of multiple reservoir sections. The corresponding type curves were developed, and sensitivity analysis was carried out.

[15] studied the expression of pressure distribution was determined. They developed ten models for pressure distribution in horizontal wells as part of their research. To create such models for pressure distribution for horizontal wells under different boundary variations, they used source functions and the Newman product rule.The derivation of 10 pressure distribution models for horizontal well using Source function has been carried out and the results are presented as follows: Completely Bounded Reservoir: The derived model for pressure distribution for completely bounded reservoir. Along the x-axis this model has infinite-slab sources, along the y-axis it has infinite plane sources and z-axis it has infinite-plane sources. Bottom water and all others infinite acting: The derived model for pressure distribution for reservoir subjected to bottom water and infinite acting. Along the x-axis it has infinite sources, along the y-axis it has infinite sources and along the z-axis it has infinite-plane sources in infinite-slab sources.

[16] studied the varying geological and structural configuration of various naturally fractured reservoirs, they have made several attempts at classifying them into different types with similar characteristics. This work presents a critical review to provide into what knowledge has been gained thus far, and what limitations are inherent in the existing models and how best to improve them. Pressure transient analysis review of flow in reservoirs having natural fractures, vugs and caves was presented to provide an insight into how much knowledge has been acquired about this phenomenon and to highlight the gaps still open for further research. They applied continuity equation, Darcy's Law and pressure diffusivity equation relating the matrix and fracture. Warren and Root(1963) presented a model utilizing the concept of mathematical superposition. 2D-solute diffusivity problem was solved by using finite -element analysis. Finite-element method, finite-difference method and finite-volume method have served as an extension of the discrete model technique.

[15] developed a two-phase model to simulate the pressure transient behavior of a water injection well in a multi well system. They discussed the influence of the saturation gradients and interference from adjacent injectors on the pressure transient behavior of the testing injector. Finite volume method was used to discretize partially differential flow equations in a hybrid grid system. Implicit Newton-Raphson method was also employed to solve equations in the model. The type curve of a falloff test with the interference of two adjacent injectors is generated from two-phase numerical model.
[15] studied the distribution of pressure in a bounded circular reservoir. In this study, they predicted the pressure distribution for the whole reservoir. Finite element method was used to approximate the values of well pressure in the entire bounded circular reservoir. The results obtained was dimensionless pressure and dimensionless time, and the relationship between them was linear. The dimensionless radii obtained are 1.5, 2 ,2.5, 3, 3.5, 4, 5, 6, 7, 8, 9 and 10.
[17] investigate the performance of a horizontal well in anisotropic reservoir when all the boundaries are sealed. They formulate a mathematical model that can be used to approximate pressure response in a horizontal well and a mathematical analysis can be used to obtain well and reservoir parameters. They study the effect of rectangular drainage with sealed boundaries. Source and Green's function was used to formulate mathematical model for dimensionless pressure. The plot of pressure derivative against the square root of time derivative gives a straight line, whose slope was used to estimate anisotropic ratio in the direction perpendicular to the well.

4. Mathematical Model Description

4.1. Diffusivity Equation

Unsteady flow of fluids is governed by diffusivity equation. This is a three-dimensional partial differential equation of the heterogeneous type that describes the flow of oil through porous media for various boundary conditions given by Odeh and Babu (1989) as.

$$k\frac{\partial^2 P}{\partial x^2} + k\frac{\partial^2 P}{\partial y^2} + k\frac{\partial^2 P}{\partial z^2} = \phi\mu c_t \frac{\partial P}{\partial t} \tag{1}$$

where k is the formation permeability. Formation permeability is equal to the axial permeability in the x, y, z directions since the reservoir is assumed to be homogeneous and isotropic, ϕ is the porosity, μ is the reservoir fluid viscosity, c_t is total compressibility and P is pressure. The solution of this equation,which gives pressure response is obtained using initial and boundary conditions and by the use of instantaneous source and Green's functions as defined by Gringarten and Ramey (1973). The solution is then expressed in dimensionless form as dimensionless pressure, P_D and its derivative $P_D^{'}$ defined.

4.2. Source and Green's Function

An infinite-slab source of Length L located at $x = x_w$ in an infinite-slab reservoir given by.

$$S(x_D,\tau_D) = \frac{1}{2}[erf(\frac{\sqrt{\frac{k}{k_x}} + (x_D - x_{wD})}{2\sqrt{\tau_D}}) + erf(\frac{\sqrt{\frac{k}{k_x}} + (x_D - x_{wD})}{2\sqrt{\tau_D}})] \tag{2}$$

for early time approximation.

$$S(x_D,\tau_D) = \frac{1}{x_{eD}}[1 + \frac{2x_{eD}}{\pi}\sum_{n=1}^{\infty}\frac{1}{n}\exp(-\frac{n^2\pi^2\tau_D}{x_{eD}^2})\sin\frac{n\pi}{x_{eD}}\cos\frac{n\pi x_{wD}}{x_{eD}}\cos\frac{n\pi x_D}{x_{eD}}] \tag{3}$$

for late time approximation.

An infinite Plane-Source located at $y = y_w$ in an infinite-slab reservoir of width y_e given by.

$$S(y_D,\tau_D) = \frac{1}{2\sqrt{\pi t_D}}\sqrt{\frac{k}{k_y}}[\exp(-\frac{(y_D - y_{wD})^2}{4\tau_D})] \tag{4}$$

for early time approximation.

$$S(y_D,\tau_D) = \frac{1}{y_{eD}}[1 + 2\sum_{m=1}^{\infty}\exp(-\frac{m^2\pi^2\tau_D}{y_{eD}^2})\cos\frac{m\pi y_{wD}}{y_{eD}}\cos\frac{m\pi y_D}{y_{eD}}] \tag{5}$$

for late time Approximation.
An infinite plane-source at $z = z_w$ in an infinite-slab reservoir of thickness h given by.

$$S(z_D,\tau_D) = \frac{1}{2\sqrt{\pi t_D}}\sqrt{\frac{k}{k_z}}[\exp(-\frac{(z_D - z_{wD})^2}{4\tau_D})] \tag{6}$$

for early time approximation.

$$S(z_D,\tau_D) = \frac{1}{h_D}[1 + 2\sum_{l=1}^{\infty}\exp(-\frac{l^2\pi^2\tau_D}{h_D^2})\cos\frac{l\pi z_{wD}}{h_D}\cos\frac{l\pi z_D}{h_D}] \tag{7}$$

for late time approximation.
where$S(x_D,\tau_D)$, $S(y_D,\tau_D)$, and $S(z_D,\tau_D)$ are the dimensionalised forms of Source and Green's functions. Therefore dimensionless pressure P_D becomes.

$$P_D = 2\pi h_D\int_0^{t_D} S(x_D,\tau_D)\times S(y_D,\tau_D)\times S(z_D,\tau_D)d\tau_D \tag{8}$$

4.3. Odeh and Babu Strategies of Delineating Flow Periods (Odeh and Babu, 1989)

The analysis of horizontal wells is considered to be more complex compared to that of vertical wells. This is due to the three dimensional geometry that has to be considered for horizontal wells. Unlike vertical wells which consider an infinite-acting radial flow period, horizontal wells can have several flow periods depending on the reservoir's horizontal dimensions and formation thickness. Odeh and Babu (1989) made an attempt to determine the number of flow periods that can occur in a horizontal well. In this study we apply the method presented by Odeh and Babu who suggested four flow periods: early radial, early linear, pseudo radial and late linear. Apart from the four listed, we also studied pseudo steady state flow.

5. Integration of Flow Regimes

5.1. Early Radial

$$P_D = 2\pi h_D \int_0^{t_{D1}} \{\frac{1}{2} erf(\frac{\sqrt{\frac{k}{k_x}} + (x_D - x_{wD})}{2\sqrt{t_D}}) + erf(\frac{\sqrt{\frac{k}{k_x}} + (x_D - x_{wD})}{2\sqrt{t_D}}) \times \frac{1}{2\sqrt{\pi t_D}}[\sqrt{\frac{k}{k_y}} e^{-\frac{(y_D - y_{wD})^2}{4t_D}}] \times \frac{1}{2\sqrt{\pi t_D}}[\sqrt{\frac{k}{k_z}} e^{-\frac{(z_D - z_{wD})^2}{4t_D}}]\} d\tau_D \quad (9)$$

$$\beta = erf(\frac{\sqrt{\frac{k}{k_x}} + (x_D - x_{wD})}{2\sqrt{\tau_D}}) + erf(\frac{\sqrt{\frac{k}{k_x}} + (x_D - x_{wD})}{2\sqrt{\tau_D}}) \quad (10)$$

$\beta = 2$, when $\sqrt{\frac{k}{k_x}} > x_D$, since the reservoir is assumed to be homogeneous and isotropic.

$$P_D = 2\pi h_D \int_0^{t_{D1}} \{\frac{1}{2\sqrt{\pi t_D}}[\sqrt{\frac{k}{k_y}} e^{-\frac{(y_D - y_{wD})^2}{4t_D}}] \times \frac{1}{2\sqrt{\pi t_D}}[\sqrt{\frac{k}{k_z}} e^{-\frac{(z_D - z_{wD})^2}{4t_D}}]\} d\tau_D \quad (11)$$

$$Ei(-x) = \int_x^{\infty} \frac{e^- u}{u} du \quad (12)$$

$$u = \frac{r_{wD}^2}{4t_D} \quad where \quad r_{wD^2} = (y_D - y_{wD})^2 + (z_D - z_{wD})^2 \quad (13)$$

$$P_D = -\frac{h_D}{4} Ei(-\frac{r_{wD^2}}{4t_D}) \quad (14)$$

where $h_D = \frac{1}{L_D}$

$$P_D = -\frac{1}{4L_D} Ei(-\frac{r_{wD^2}}{4_{tD}}) \quad (15)$$

$$P_D^{'} = \frac{1}{4L_D} exp(-\frac{r_{wD^2}}{4t_D}) \quad (16)$$

5.2. Early Linear

$$P_D = 2\pi h_D \int_{t_{D1}}^{t_{D2}} \{\frac{1}{2}[erf(\frac{\sqrt{\frac{k}{k_x}} + (x_D - x_{wD})}{2\sqrt{t_D}}) + erf(\frac{\sqrt{\frac{k}{k_x}} + (x_D - x_{wD})}{2\sqrt{t_D}})] \times \frac{1}{2\sqrt{\pi t_D}}\sqrt{\frac{k}{k_y}} \exp[-\frac{(y_D - y_{wD})^2}{4t_D}] \times \frac{1}{h_D}[1 + 2\sum_{l=1}^{\infty} \exp(-\frac{l^2\pi^2\tau_D}{h_D^2}) \cos\frac{l\pi z_{wD}}{h_D} \cos\frac{l\pi z_D}{h_D}]\} d\tau_D \quad (17)$$

$$P_D = 2\pi h_D \int_{t_{D1}}^{t_{D2}} \{\frac{1}{2}[erf(\frac{\sqrt{\frac{k}{k_x}} + (x_D - x_{wD})}{2\sqrt{t_D}}) + erf(\frac{\sqrt{\frac{k}{k_x}} + (x_D - x_{wD})}{2\sqrt{t_D}})] \times \frac{1}{2\sqrt{\pi t_D}}\sqrt{\frac{k}{k_y}} \exp[(-\frac{y_D - y_{wD}^2}{4t_D})] \times \frac{1}{h_D}[1 + 2\sum_{l=1}^{\infty} \exp(-\frac{l^2\pi^2\tau_D}{h_D^2}) \cos\frac{l\pi z_{wD}}{h_D} \cos\frac{l\pi z_D}{h_D}]\} d\tau_D \quad (18)$$

$$\beta = erf(\frac{\sqrt{\frac{k}{k_x}} + (x_D - x_{wD})}{2\sqrt{\tau_D}}) + erf(\frac{\sqrt{\frac{k}{k_x}} + (x_D - x_{wD})}{2\sqrt{\tau_D}}) \tag{19}$$

For $\beta = 2$ since $\sqrt{\frac{k}{k_x}} > x_D$, because the reservoir is assumed to be homogenous and isotropic.
$l = m = n = 1$.
A line source is considered such that $y_D = y_{wD}$ and $r_{wD} = z_D - z_{wD}$.
A monitoring point at the center of the well is considered such that $x_D = x_{wD}$.

$$P_D = \frac{\pi}{\sqrt{\pi t_D}} \int_{t_{D1}}^{t_{D2}} [1 + 2\sum_{l=1}^{1} \exp(-\frac{l^2\pi^2\tau_D}{h_D^2}) \cos\frac{l\pi z_{wD}}{h_D} \cos\frac{l\pi z_D}{h_D}] d\tau_D \tag{20}$$

$z = h$, $z_D = h_D$, $z = z_w$, $z_D = z_{wD} = h_D$

$$P_D = \sqrt{\pi} \int_{t_{D1}}^{t_{D2}} 1 + 2exp(-\frac{\pi^2\tau_D}{h_{D^2}}) \frac{d\tau_D}{\sqrt{\tau_D}} \tag{21}$$

$$P_D = \sqrt{\pi} \int_{tD_1}^{t_{D2}} (1 + 2e^{-}\frac{\pi^2}{h_{D^2}}\tau_D) \frac{d\tau_D}{\sqrt{\tau_D}} \tag{22}$$

$$P_D = \sqrt{\pi}[\sqrt{t_D} - 2\frac{h_{D^2}}{\pi^2} e^{-}\frac{\pi^2}{h_{D^2}}\sqrt{t_D}] \tag{23}$$

Now by substituting the upper and the lower bounds.

$$P_D = \sqrt{\pi}\{[\sqrt{t_{D2}} - 2\frac{h_{D^2}}{\pi^2} e^{-}\frac{\pi^2}{h_{D^2}}\sqrt{t_{D2}}] - [\sqrt{t_{D1}} - 2\frac{h_{D^2}}{\pi^2} e^{-}\frac{\pi^2}{h_{D^2}}\sqrt{t_{D1}}]\} \tag{24}$$

$$P_D = \sqrt{\pi}[\sqrt{t_{D2}} - \sqrt{t_{D1}} - 2\frac{h_{D^2}}{\pi^2} e^{-}\frac{\pi^2}{h_{D^2}}\sqrt{t_{D2}} + 2\frac{h_{D^2}}{\pi^2} e^{-}\frac{\pi^2}{h_{D^2}}\sqrt{t_{D1}}] \tag{25}$$

$$P_{D'} = t_D \frac{\partial P_D}{\partial t_D} \tag{26}$$

$$P_{D'} = \sqrt{\pi}[1 + 2exp(-\frac{\pi^2\tau_D}{h_{D^2}})]\sqrt{t_D} \tag{27}$$

$$P_{D'} = \sqrt{\pi t_D}[1 + 2e^{-}\frac{\pi^2\tau_D}{h_{D^2}}\sqrt{t_D}] \tag{28}$$

5.3. pseudoradial

$$P_D = 2\pi h_D \int_{t_{D2}}^{t_{D3}} \{\frac{1}{2}[erf(\frac{\sqrt{\frac{k}{k_x}} + (x_D - x_{wD})}{2\sqrt{t_D}}) + erf(\frac{\sqrt{\frac{k}{k_x}} + (x_D - x_{wD})}{2\sqrt{t_D}})]$$
$$\times \frac{1}{y_{eD}}[1 + 2\sum_{m=1}^{\infty}(-\frac{m^2\pi^2\tau_D}{y_{eD}^2}) \cos\frac{m\pi y_{wD}}{y_{eD}} \cos\frac{m\pi y_D}{y_{eD}}]$$
$$\times \frac{1}{h_D}[1 + 2\sum_{l=1}^{\infty} \exp(-\frac{l^2\pi^2\tau_D}{h_D^2}) \cos\frac{l\pi z_{wD}}{h_D} \cos\frac{l\pi z_D}{h_D}]\} d\tau_D \tag{29}$$

For $\beta = 2$ since $\sqrt{\frac{k}{k_x}} > x_D$, because the reservoir is assumed to be homogenous and isotropic.
$l = m = n = 1$

A line source is considered such that $y_D = y_{wD}$ and $r_{wD} = z_D - z_{wD}$.
A monitoring point at the center of the well is considered such that $x_D = x_{wD}$.

$$P_D = \frac{2\pi}{y_{eD}} \int_{t_{D2}}^{t_{D3}} [1 + 2\sum_{m=1}^{1} \exp(-\frac{\pi^2 \tau_D}{y_{eD}^2}) \cos\frac{\pi y_{wD}}{y_{eD}} \cos\frac{\pi y_D}{y_{eD}}] \times [1 + 2\sum_{l=1}^{1} \exp(-\frac{\pi^2 \tau_D}{h_{D^2}}) \cos\frac{\pi z_{wD}}{h_D} \cos\frac{\pi z_D}{h_D}] d\tau_D \quad (30)$$

$$P_D = \frac{2\pi}{y_{eD}} \int_{t_{D2}}^{t_{D3}} [(1 + 2\exp(-\frac{\pi^2 \tau_D}{y_{eD}^2}) \cos\frac{\pi y_{wD}}{y_{eD}} \cos\frac{\pi y_D}{y_{eD}}) * (1 + 2\exp(-\frac{\pi^2 \tau_D}{h_D^2}) \cos\frac{\pi z_{wD}}{h_D} \cos\frac{\pi z_D}{h_D})] d\tau_D \quad (31)$$

$r_{wD} = z_D - z_{wD}$
$x_D = x_{wD}$
$y_D = y_{wD}$
$y_{eD} = 2y_D = 2y_{wD}$

$$P_D = \frac{2\pi}{y_{eD}} \int_{t_{D2}}^{t_{D3}} [(1 + 2\exp(-\frac{\pi^2 \tau_D}{y_{eD}^2}) \cos\frac{\pi}{2} \cos\frac{\pi}{2}) * (1 + 2\exp(-\frac{\pi^2 \tau_D}{h_D^2}) \cos\frac{\pi z_{wD}}{h_D} \cos\frac{\pi z_D}{h_D})] d\tau_D \quad (32)$$

$$P_D = \frac{2\pi}{y_{eD}} \int_{t_{D2}}^{t_{D3}} [(1 + 2\exp(-\frac{\pi^2 \tau_D}{y_{eD}^2})0) * (1 + 2\exp(-\frac{\pi^2 \tau_D}{h_D^2}) \cos\frac{\pi z_{wD}}{h_D} \cos\frac{\pi z_D}{h_D})] d\tau_D \quad (33)$$

$z = h$, $z_D = h_D$, $z = z_w$, $z_D = z_{wD} = h_D$

$$P_D = \frac{2\pi}{y_{eD}} \int_{t_{D2}}^{t_{D3}} (1 * (1 + 2\exp(-\frac{\pi^2 \tau_D}{h_D^2}) \cos\pi \cos\pi)) d\tau_D \quad (34)$$

$$P_D = \frac{2\pi}{y_{eD}} \int_{t_{D2}}^{t_{D3}} (1 + 2\exp(-\frac{\pi^2 \tau_D}{h_D^2})) d\tau_D \quad (35)$$

$$P_D = \frac{2\pi}{y_{eD}} \int_{t_{D2}}^{t_{D3}} (1 + 2e^{-} \frac{\pi^2}{h_D^2} \tau_D) d\tau_D \quad (36)$$

$$P_D = \frac{2\pi}{y_{eD}} [t_D - 2\frac{h_D^2}{\pi^2} e^{-} \frac{\pi^2}{h_D^2} t_D] \quad (37)$$

Now by substituting the bounds, we get.

$$P_D = \frac{2\pi}{y_{eD}} \{[t_{D3} - 2\frac{h_D^2}{\pi^2} e^{-} \frac{\pi^2}{h_D^2} t_{D3}] - [t_{D2} - 2\frac{h_{D^2}}{\pi^2} e^{-} \frac{\pi^2}{h_D^2} t_{D2}]\} \quad (38)$$

$$P_D = \frac{2\pi}{y_{eD}} [t_{D3} - t_{D2} - 2\frac{h_{D^2}}{\pi^2} e^{-} \frac{\pi^2}{h_{D^2}} t_{D3} + 2\frac{h_D^2}{\pi^2} e^{-} \frac{\pi^2}{h_{D^2}} t_{D2}] \quad (39)$$

$$P_D^{'} = t_D \frac{\partial P_D}{\partial t_D} \quad (40)$$

$$P_D^{'} = \frac{2\pi t_D}{y_{eD}} (1 + 2e^{-} \frac{\pi^2}{h_{D^2}} \tau_D) \quad (41)$$

5.4. Late Linear

$$P_D = \frac{2\pi}{x_{eD}y_{eD}}\int_{t_{D3}}^{t_D}\{[1+\frac{2x_{eD}}{\pi}\sum_{n=1}^{\infty}\frac{1}{n}\exp(-\frac{n^2\pi^2\tau_D}{x_{eD}^2})\sin\frac{n\pi}{x_{eD}}\cos\frac{n\pi x_{wD}}{x_{eD}}\cos\frac{n\pi x_D}{x_{eD}}]$$
$$\times[1+2\sum_{m=1}^{\infty}\exp(-\frac{m^2\pi^2\tau_D}{y_{eD}^2})\cos\frac{m\pi y_{wD}}{y_{eD}}\cos\frac{m\pi y_D}{y_{eD}}]$$
$$\times[1+2\sum_{l=1}^{\infty}\exp(-\frac{l^2\pi^2\tau_D}{h_D^2})\cos\frac{l\pi z_{wD}}{h_D}\cos\frac{l\pi z_D}{h_D}]\}d\tau_D \quad (42)$$

$l = m = n = 1$
A line source is considered such that $y_D = y_{wD}$ and $r_{wD} = z_D - z_{wD}$.
A monitoring point at the center of the well is considered such that $x_D = x_{wD}$.

$$P_D = \frac{2\pi}{x_{eD}y_{eD}}\int_{t_{D3}}^{t_D}\{[1+\frac{2x_{eD}}{\pi}\sum_{n=1}^{1}\exp(-\frac{\pi^2\tau_D}{x_{eD}^2})\sin\frac{\pi}{x_{eD}}\cos\frac{\pi x_{wD}}{x_{eD}}\cos\frac{\pi x_D}{x_{eD}}]$$
$$\times[1+2\sum_{m=1}^{1}\exp(-\frac{\pi^2\tau_D}{y_{eD^2}})\cos\frac{\pi y_{wD}}{y_{eD}}\cos\frac{\pi y_D}{y_{eD}}]$$
$$\times[1+2\sum_{l=1}^{1}\exp(-\frac{\pi^2\tau_D}{h_{D^2}})\cos\frac{\pi z_{wD}}{h_D}\cos\frac{\pi z_D}{h_D}]\}d\tau_D \quad (43)$$

$$P_D = \frac{2\pi}{x_{eD}y_{eD}}\int_{t_{D3}}^{t_D}[(1+\frac{2x_{eD}}{\pi}\exp(-\frac{\pi^2\tau_D}{x_{eD}^2})\sin\frac{\pi}{x_{eD}}\cos\frac{\pi x_{wD}}{x_{eD}}\cos\frac{\pi x_D}{x_{eD}})$$
$$*(1+2\exp(-\frac{\pi^2\tau_D}{y_{eD^2}})\cos\frac{\pi y_{wD}}{y_{eD}}\cos\frac{\pi y_D}{y_{eD}})$$
$$*(1+2\exp(-\frac{\pi^2\tau_D}{h_{D^2}})\cos\frac{\pi z_{wD}}{h_D}\cos\frac{\pi z_D}{h_D})]d\tau_D \quad (44)$$

$r_{wD} = z_D - z_{wD}$
$x_D = x_{wD}$
$y_D = y_{wD}$
$x_{eD} = 2x_D = 2x_{wD}$
$y_{eD} = 2y_D = 2y_{wD}$

$$P_D = \frac{2\pi}{x_{eD}y_{eD}}\int_{t_{D3}}^{t_D}[(1+\frac{2x_{eD}}{\pi}\exp(-\frac{\pi^2\tau_D}{x_{eD^2}})\sin\frac{\pi}{x_{eD}}\cos\frac{\pi}{2}\cos\frac{\pi}{2})$$
$$*(1+2\exp(-\frac{\pi^2\tau_D}{y_{eD^2}})\cos\frac{\pi}{2}\cos\frac{\pi}{2})$$
$$*(1+2\exp(-\frac{\pi^2\tau_D}{h_{D^2}})\cos\frac{\pi z_{wD}}{h_D}\cos\frac{\pi z_D}{h_D})]d\tau_D \quad (45)$$

$$P_D = \frac{2\pi}{x_{eD}y_{eD}}\int_{t_{D3}}^{t_D}[1*(1+2\exp(-\frac{\pi^2\tau_D}{h_{D^2}})\cos\frac{\pi z_{wD}}{h_D}\cos\frac{\pi z_D}{h_D})]d\tau_D \quad (46)$$

$z = h$, $z_D = h_D$, $z = z_w$, $z_D = z_{wD} = h_D$

$$P_D = \frac{2\pi}{x_{eD}y_{eD}}\int_{t_{D3}}^{t_D}(1+2\exp(-\frac{\pi^2\tau_D}{h_{D^2}})\cos\pi\cos\pi)d\tau_D \quad (47)$$

$$P_D = \frac{2\pi}{x_{eD}y_{eD}}\int_{t_{D3}}^{t_D}(1+2\exp(-\frac{\pi^2\tau_D}{h_{D^2}}))d\tau_D \quad (48)$$

$$P_D = \frac{2\pi}{x_{eD} y_{eD}} \int_{t_{D3}}^{t_D} (1 + 2e^{-} \frac{\pi^2}{h_{D^2}} \tau_D) d\tau_D \tag{49}$$

$$P_D = \frac{2\pi}{x_{eD} y_{eD}} [t_D - 2\frac{h_{D^2}}{\pi^2} e^{-} \frac{\pi^2}{h_{D^2}} t_D] \tag{50}$$

Now by substituting the bounds.

$$P_D = \frac{2\pi}{x_{eD} y_{eD}} \{[t_D - 2\frac{h_{D^2}}{\pi^2} e^{-} \frac{\pi^2}{h_{D^2}} t_D] - [t_{D3} - 2\frac{h_{D^2}}{\pi^2} e^{-} \frac{\pi^2}{h_{D^2}} t_{D3}]\} \tag{51}$$

$$P_D = \frac{2\pi}{x_{eD} y_{eD}} [t_D - t_{D3} - 2\frac{h_{D^2}}{\pi^2} e^{-} \frac{\pi^2}{h_{D^2}} t_D + 2\frac{h_{D^2}}{\pi^2} e^{-} \frac{\pi^2}{h_{D^2}} t_{D3}] \tag{52}$$

$$P_D^{'} = t_D \frac{\partial P_D}{\partial t_D} \tag{53}$$

$$P_D^{'} = \frac{2\pi t_D}{x_{eD} y_{eD}} (1 + 2e^{-} \frac{\pi^2}{h_{D^2}} \tau_D) \tag{54}$$

6. Tables and figures

From the previous section, we considered a theoretical well, reservoir parameters and substituted them in the final models obtained as indicated by equations (15), (16), (25), (28).(39), (40), (52)and(54) were implemented in MATLAB version ($R2021b$) to compute the dimensionless pressure and its derivatives. We analysed the effects of the well and reservoir parameters on the well performance using log-log plots. The various parameters that have been varied includes the length of the well, dimensionless length of the well, dimensionless height, dimensionless width, dimensionless source coordinate in the x-direction, dimensionless source coordinate in the y-direction, dimensionless source coordinate in the z-direction, dimensionless reservoir length, dimensionless reservoir width, dimensionless reservoir height and dimensionless well bore radius. The results are presented in tables and graphs.

parameters with varying L_D

$k = k_x = k_y = k_z = 20md$, $h = 75ft$, $x_e = 5000ft$, $y_e = 3500ft$, $z_e = 2000$, $z_w = 400ft$ and z=450md

Table 1. parameters with varying L_D

$L(ft)$	500	1000	1500	2000	2500	3000	3500	4000	4500	5000
L_D	3.333	6.667	10.000	13.333	16.667	20.000	23.333	26.667	30.000	33.333
h_D	0.300	0.150	0.100	0.075	0.060	0.050	0.043	0.038	0.033	0.030
x_D	0.5	0.5	0.5	0.5	0.5	0.5	0.5	0.5	0.5	0.5
y_D	7.000	3.500	2.334	1.750	1.400	1.167	1.000	0.875	0.778	0.700
z_D	1.800	0.900	0.600	0.450	0.360	0.300	0.257	0.225	0.200	0.180
x_{wD}	0.5	0.5	0.5	0.5	0.5	0.5	0.5	0.5	0.5	0.5
y_{wD}	7.000	3.500	2.334	1.750	1.400	1.167	1.000	0.875	0.778	0.700
z_{wD}	1.600	0.800	0.533	0.400	0.320	0.267	0.229	0.200	0.178	0.160
x_{eD}	20.000	10.000	6.667	5.000	4.000	3.333	2.857	2.500	2.222	2.000
y_{eD}	14.000	7.000	4.667	3.500	2.800	2.333	2.000	1.750	1.556	1.400
z_{eD}	8.000	4.000	2.667	2.000	1.600	1.333	1.143	1.000	0.889	0.800
r_{wD}	0.200	0.100	0.067	0.050	0.040	0.033	0.028	0.025	0.022	0.020

The dimensionless reservoir width, y_{eD} and dimensionless pay thickness, h_D varies inversely as dimensionless well length, L_D.

7. Early Linear Flow

Dimensionless pressure and dimensionless pressure derivative with an increased in dimensionless time.

7.1. Table of Early Linear Flow

Table 2 clearly shows that as dimensionless time, t_{D2} increases both dimensionless pressure, P_D and dimensionless pressure derivative, $P_{D'}$ also increases but the values of dimensionless pressure derivative are larger than dimensionless pressure. Early linear flow shows that dimensionless time is directly proportional to both dimensionless pressure and dimensionless pressure derivative. This was the case when x and y-boundaries are infinite acting while z-boundary has been felt.

7.2. Graphs of Early Linear Flow Period

Figure 3 and 4 is the graph of dimensionless pressure and dimensionless pressure derivative against dimensionless time, it was observed from log-log plot as dimensionless time increases both the dimensionless pressure and dimensionless pressure derivative increased

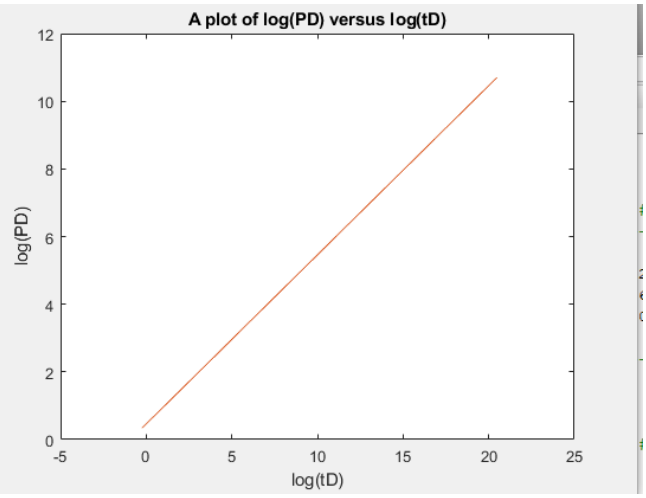

Fig. 2. Dimensionless pressure grows with dimensionless time

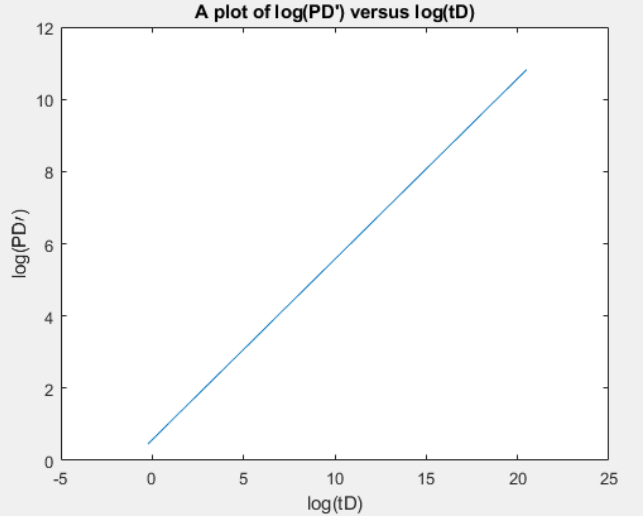

Fig. 3. Dimensionless pressure derivative grows with dimensionless time

8. Pseudo radial Flow Period

Dimensionless pressure, P_D and dimensionless pressure derivative, $P_{D'}$ for varying dimensionless reservoir width, y_{eD}

We observed that from Table 3 to Table 12, as dimensionless reservoir width, y_{eD} decreases both dimensionless pressure, P_D and dimensionless pressure derivative, $P_{D'}$ increases during pseudoradial flow period. Dimensionless reservoir width, y_{eD} is inversely proportional to both the dimensionless pressure and dimensionless pressure derivative. During pseudoradial flow period both the dimensionless pressure and dimensionless pressure derivative grows with dimensionless time.

8.1. Graphs of pseudoradial flow

Figure 4.4 and 4.5 is the graph of dimensionless pressure against dimensionless time and dimensionless pressure derivative against dimensionless time, it has shown clearly on the log-log plots that as dimensionless pressure increases, dimensionless pressure derivative increases, dimensionless time increases and dimensionless width also increases.

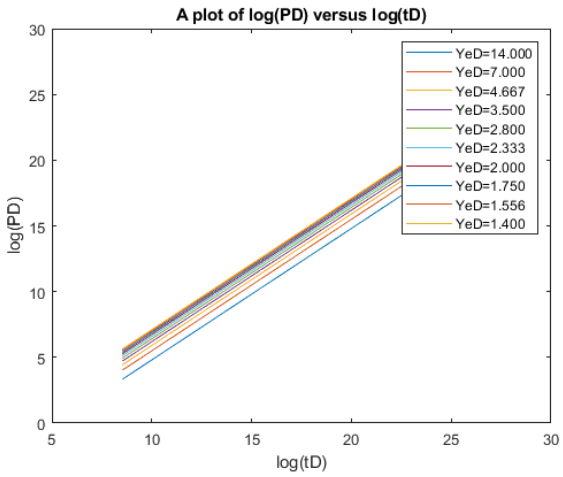

Fig. 4. Dimensionless pressure grows with dimensionless time

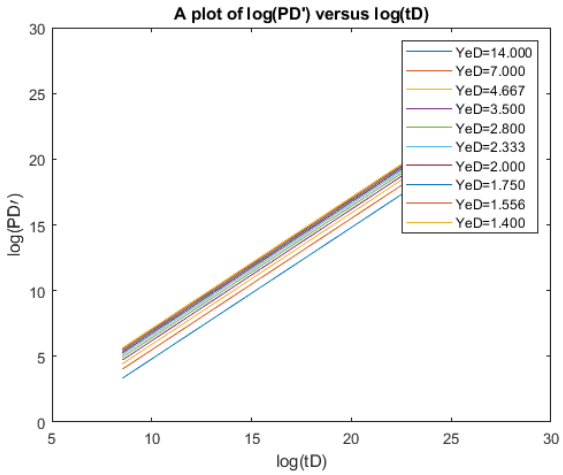

Fig. 5. Dimensionless pressure derivative grows with dimensionless time

9. Late Linear Flow

9.1. Tables of Late Linear Flow

It is also clearly showed that from Table 13 to Table 22 as dimensionless reservoir length, x_{eD} decreases both dimensionless pressure, P_D and dimensionless pressure derivative, $P_{D'}$ increases which implies that dimensionless reservoir length is inversely proportional to both dimensionless pressure and dimensionless pressure derivative. This is the time when all the boundaries of the reservoir has been affected by the flow, that is the pressure approximation

at all the boundaries is a late time.

9.2. Graphs of Late Linear Flow

Figure 7 and 8 is the graph of dimensionless pressure against dimensionless time and dimensionless pressure derivative against time, the log-log plot shows that as dimensionless pressure increases, dimensionless pressure derivative increases, dimensionless time increases and dimensionless reservoir length also increases.

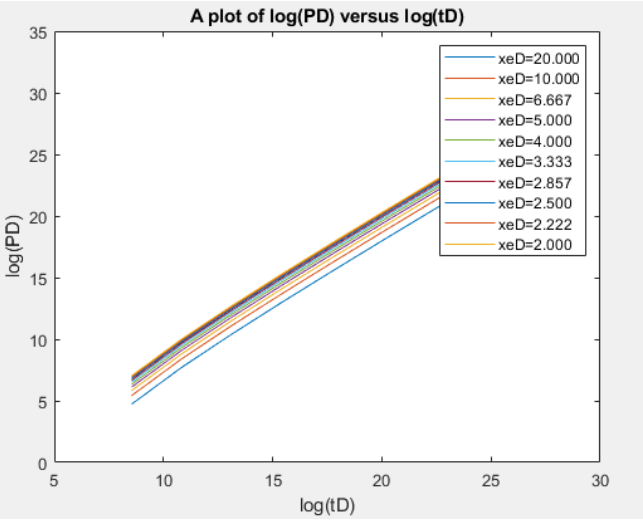

Fig. 6. Dimensionless pressure grows with dimensionless time

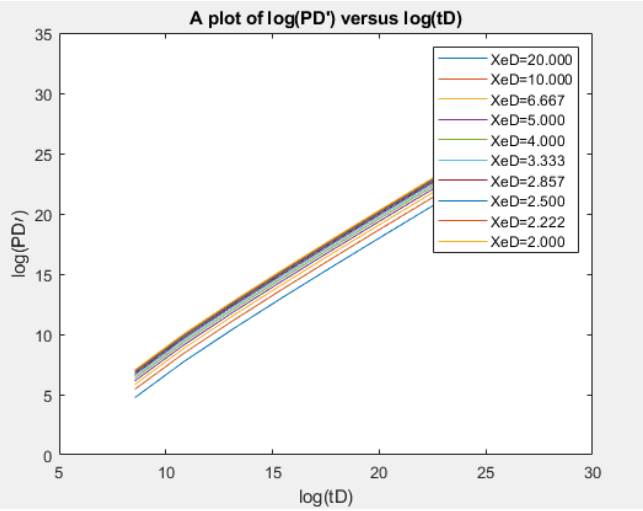

Fig. 7. Dimensionless derivative pressure grows with dimensionless time

Table 2. The values of P_D and $P_{D'}$ with an increased t_D

t_{D2}	P_D	$P_{D'}$
7.9×10^{-01}	1.408086	1.575391
7.9×10^{00}	4.452757	4.981825
7.9×10^{01}	14.080855	15.753914
7.9×10^{02}	44.527574	49.818252
7.9×10^{03}	140.808553	157.539144
7.9×10^{04}	445.275743	498.182516
7.9×10^{05}	1408.085534	1575.391442
7.9×10^{06}	4452.757428	4981.825164
7.9×10^{07}	14080.855340	15753.914423
7.9×10^{08}	44527.574276	49818.251639

Table 3. The values of P_D and $P_{D'}$ when $y_{eD} = 14.0000$

t_{D3}	P_D	$P_{D'}$
6.4×10^{01}	28.364094	28.364094
6.4×10^{02}	283.640937	283.640937
6.4×10^{03}	2836.409367	2836.409367
6.4×10^{04}	28364.093672	28364.093672
6.4×10^{05}	283640.936724	283640.936724
6.4×10^{06}	2836409.367241	2836409.367241
6.4×10^{07}	28364093.672411	28364093.672411
6.4×10^{08}	283640936.724107	283640936.724107
6.4×10^{09}	2836409367.241070	2836409367.241070
6.4×10^{10}	28364093672.410702	28364093672.410706

Table 4. The values of P_D and $P_{D'}$ when $y_{eD} = 7.0000$

t_{D3}	P_D	$P_{D'}$
6.4×10^{01}	56.728187	56.728187
6.4×10^{02}	567.281873	567.281873
6.4×10^{03}	5672.818734	5672.818734
6.4×10^{04}	56728.187345	56728.187345
6.4×10^{05}	567281.873448	567281.873448
6.4×10^{06}	5672818.734482	5672818.734482
6.4×10^{07}	56728187.344821	56728187.344821
6.4×10^{08}	567281873.448214	567281873.448214
6.4×10^{09}	5672818734.482141	5672818734.482141
6.4×10^{10}	56728187344.821404	56728187344.821411

Table 5. The values of P_D and $P_{D'}$ when $y_{eD} = 4.6670$

t_{D3}	P_D	$P_{D'}$
6.4×10^{01}	85.086203	85.086203
6.4×10^{02}	850.862034	850.862034
6.4×10^{03}	8508.620343	8508.620343
6.4×10^{04}	85086.203431	85086.203431
6.4×10^{05}	850862.034313	850862.034313
6.4×10^{06}	8508620.343127	8508620.343127
6.4×10^{07}	85086203.431273	85086203.431273
6.4×10^{08}	850862034.312727	850862034.312727
6.4×10^{09}	8508620343.127274	8508620343.127274
6.4×10^{10}	85086203431.272736	85086203431.272751

Table 6. The values of P_D and $P_{D'}$ when $y_{eD} = 3.5000$

t_{D3}	P_D	$P_{D'}$
6.4×10^{01}	113.456375	113.456375
6.4×10^{02}	1134.563747	1134.563747
6.4×10^{03}	11345.637469	11345.637469
6.4×10^{04}	113456.374690	113456.374690
6.4×10^{05}	1134563.746896	1134563.746896
6.4×10^{06}	11345637.468964	11345637.468964
6.4×10^{07}	113456374.689643	113456374.689643
6.4×10^{08}	1134563746.896428	1134563746.896428
6.4×10^{09}	11345637468.964281	11345637468.964281
6.4×10^{10}	113456374689.642807	113456374689.642822

Table 7. The values of P_D and $P_{D'}$ when $y_{eD} = 2.8000$

t_{D3}	P_D	$P_{D'}$
6.4×10^{01}	141.820468	141.820468
6.4×10^{02}	1418.204684	1418.204684
6.4×10^{03}	14182.046836	14182.046836
6.4×10^{04}	141820.468362	141820.468362
6.4×10^{05}	1418204.683621	1418204.683621
6.4×10^{06}	14182046.836205	14182046.836205
6.4×10^{07}	141820468.362054	141820468.362054
6.4×10^{08}	1418204683.620535	1418204683.620535
6.4×10^{09}	14182046836.205351	14182046836.205353
6.4×10^{10}	141820468362.053528	141820468362.053528

Table 8. The values of P_D and $P_{D'}$ when $y_{eD} = 2.3330$

6.4×10^{01}	170.208878	170.208878
6.4×10^{02}	1702.088776	1702.088776
6.4×10^{03}	17020.887759	17020.887759
6.4×10^{04}	170208.877588	170208.877588
6.4×10^{05}	1702088.775884	1702088.775884
6.4×10^{06}	17020887.758841	17020887.758841
6.4×10^{07}	170208877.588405	170208877.588405
6.4×10^{08}	1702088775.884054	1702088775.884054
6.4×10^{09}	17020887758.840540	17020887758.840540
6.4×10^{10}	170208877588.405396	170208877588.405426

Table 9. The values of P_D and $P_{D'}$ when $y_{eD} = 2.0000$

6.4×10^{01}	198.548656	198.548656
6.4×10^{02}	1985.486557	1985.486557
6.4×10^{03}	19854.865571	19854.865571
6.4×10^{04}	198548.655707	198548.655707
6.4×10^{05}	1985486.557069	1985486.557069
6.4×10^{06}	19854865.570687	19854865.570687
6.4×10^{07}	198548655.706875	198548655.706875
6.4×10^{08}	1985486557.068749	1985486557.068749
6.4×10^{09}	19854865570.687492	19854865570.687492
6.4×10^{10}	198548655706.874939	198548655706.874939

Table 10. The values of P_D and $P_{D'}$ when $y_{eD} = 1.7500$

6.4×10^{01}	226.912749	226.912749
6.4×10^{02}	2269.127494	2269.127494
6.4×10^{03}	22691.274938	22691.274938
6.4×10^{04}	226912.749379	226912.749379
6.4×10^{05}	2269127.493793	2269127.493793
6.4×10^{06}	22691274.937929	22691274.937929
6.4×10^{07}	226912749.379286	226912749.379286
6.4×10^{08}	2269127493.792856	2269127493.792856
6.4×10^{09}	22691274937.928562	22691274937.928562
6.4×10^{10}	226912749379.285614	226912749379.285645

Table 11. The values of P_D and $P_{D'}$ when $y_{eD} = 1.5560$

6.4×10^{01}	255.203928	255.203928
6.4×10^{02}	2552.039276	2552.039276
6.4×10^{03}	25520.392764	25520.392764
6.4×10^{04}	255203.927644	255203.927644
6.4×10^{05}	2552039.276438	2552039.276438
6.4×10^{06}	25520392.764380	25520392.764380
6.4×10^{07}	255203927.643798	255203927.643798
6.4×10^{08}	2552039276.437981	2552039276.437981
6.4×10^{09}	25520392764.379807	25520392764.379810
6.4×10^{10}	255203927643.798065	255203927643.798126

Table 12. The values of P_D and $P_{D'}$ when $y_{eD} = 1.4000$

6.4×10^{01}	283.640937	283.640937
6.4×10^{02}	2836.409367	2836.409367
6.4×10^{03}	28364.093672	28364.093672
6.4×10^{04}	283640.936724	283640.936724
6.4×10^{05}	2836409.367241	2836409.367241
6.4×10^{06}	28364093.672411	28364093.672411
6.4×10^{07}	283640936.724107	283640936.724107
6.4×10^{08}	2836409367.241070	2836409367.241070
6.4×10^{09}	28364093672.410702	28364093672.410706
6.4×10^{10}	283640936724.107056	283640936724.107056

Table 13. The values of P_D and $P_{D'}$ when $x_{eD} = 20.0000$

t_D	P_D	$P_{D'}$
5.1×10^{03}	113.456375	114.892531
5.1×10^{04}	2269.127494	2297.850627
5.1×10^{05}	34034.481373	34465.297592
5.1×10^{06}	453825.498759	459570.125325
5.1×10^{07}	5672818.734482	5744626.566564
5.1×10^{08}	68083551.035362	68945368.137076
5.1×10^{09}	794194622.827500	804247719.318987
5.1×10^{10}	9076509975.171425	9191402506.502708
5.1×10^{11}	102081571057.519241	103373742843.057465
5.1×10^{12}	1134563746896.428223	1148925313312.838623

Table 14. The values of P_D and $P_{D'}$ when $x_{eD} = 10.0000$

t_D	P_D	$P_{D'}$
5.1×10^{03}	226.912749	229.785063
5.1×10^{04}	4538.254988	4595.701253
5.1×10^{05}	68068.962745	68930.595185
5.1×10^{06}	907650.997517	919140.250650
5.1×10^{07}	11345637.468964	11489253.133128
5.1×10^{08}	136167102.070724	137890736.274151
5.1×10^{09}	1588389245.654999	1608495438.637974
5.1×10^{10}	18153019950.342850	18382805013.005417
5.1×10^{11}	204163142115.038483	206747485686.114929
5.1×10^{12}	2269127493792.856445	2297850626625.677246

Table 15. The values of P_D and $P_{D'}$ when $x_{eD} = 6.6670$

t_D	P_D	$P_{D'}$
5.1×10^{03}	340.352106	344.660361
5.1×10^{04}	6807.042129	6893.207220
5.1×10^{05}	102098.339201	103390.723241
5.1×10^{06}	1361408.425854	1378641.443903
5.1×10^{07}	17017605.323180	17233018.048790
5.1×10^{08}	204240441.084032	206825763.123071
5.1×10^{09}	2382464745.245237	2412622526.830620
5.1×10^{10}	27228168517.088421	27572828878.064224
5.1×10^{11}	306229401702.472595	310105723243.010254
5.1×10^{12}	3403521064636.053223	3446603609758.028320

Table 16. The values of P_D and $P_{D'}$ when $x_{eD} = 5.0000$

t_D	P_D	$P_{D'}$
5.1×10^{03}	453.825499	459.570125
5.1×10^{04}	9076.509975	9191.402507
5.1×10^{05}	136137.925490	137861.190370
5.1×10^{06}	1815301.995034	1838280.501301
5.1×10^{07}	22691274.937929	22978506.266257
5.1×10^{08}	272334204.141449	275781472.548302
5.1×10^{09}	3176778491.309999	3216990877.275949
5.1×10^{10}	36306039900.685699	36765610026.010834
5.1×10^{11}	408326284230.076965	413494971372.229858
5.1×10^{12}	4538254987585.712891	4595701253251.354492

Table 17. The values of P_D and $P_{D'}$ when $x_{eD} = 4.0000$

t_D	P_D	$P_{D'}$
5.1×10^{03}	567.281873	574.462657
5.1×10^{04}	11345.637469	11489.253133
5.1×10^{05}	170172.406863	172326.487962
5.1×10^{06}	2269127.493793	2297850.626626
5.1×10^{07}	28364093.672411	28723132.832821
5.1×10^{08}	340417755.176811	344726840.685378
5.1×10^{09}	3970973114.137498	4021238596.594935
5.1×10^{10}	45382549875.857124	45957012532.513542
5.1×10^{11}	510407855287.596130	516868714215.287292
5.1×10^{12}	5672818734482.140625	5744626566564.193359

Table 18. The values of P_D and $P_{D'}$ when $x_{eD} = 3.3330$

t_D	P_D	$P_{D'}$
5.1×10^{03}	680.806329	689.424130
5.1×10^{04}	13616.126575	13788.482608
5.1×10^{05}	204227.310966	206812.466801
5.1×10^{06}	2723225.315083	2757696.521603
5.1×10^{07}	34040316.438537	34471206.520037
5.1×10^{08}	408542160.428216	413713580.180472
5.1×10^{09}	4765644301.395138	4825968912.805202
5.1×10^{10}	54464506301.658707	55153930432.059448
5.1×10^{11}	612550681413.256836	620304487507.095459
5.1×10^{12}	6808063287707.339844	6894241304007.432617

Table 19. The values of P_D and $P_{D'}$ when $x_{eD} = 2.8570$

t_D	P_D	$P_{D'}$
5.1×10^{03}	794.234335	804.287934
5.1×10^{04}	15884.686691	16085.758674
5.1×10^{05}	238253.282272	241269.146604
5.1×10^{06}	3176937.338177	3217151.734863
5.1×10^{07}	39711716.727211	40214396.685784
5.1×10^{08}	476608687.681919	482641709.044981
5.1×10^{09}	5559640341.809588	5630015536.009709
5.1×10^{10}	63538746763.538139	64343034697.253815
5.1×10^{11}	714606727739.021484	723652382520.528198
5.1×10^{12}	7942343345442.268555	8042879337156.727539

Table 20. The values of P_D and $P_{D'}$ when $x_{eD} = 2.5000$

t_D	P_D	$P_{D'}$
5.1×10^{03}	907.650998	919.140251
5.1×10^{04}	18153.019950	18382.805013
5.1×10^{05}	272275.850980	275722.380739
5.1×10^{06}	3630603.990069	3676561.002601
5.1×10^{07}	45382549.875857	45957012.532514
5.1×10^{08}	544668408.282897	551562945.096605
5.1×10^{09}	6353556982.619998	6433981754.551897
5.1×10^{10}	72612079801.371399	73531220052.021667
5.1×10^{11}	816652568460.153931	826989942744.459717
5.1×10^{12}	9076509975171.425781	9191402506502.708984

Table 21. The values of P_D and $P_{D'}$ when $x_{eD} = 2.2220$

t_D	P_D	$P_{D'}$
5.1×10^{03}	1021.209493	1034.136196
5.1×10^{04}	20424.189863	20682.723912
5.1×10^{05}	306340.966449	310218.700202
5.1×10^{06}	4084837.972624	4136544.782404
5.1×10^{07}	51060474.657805	51706809.780056
5.1×10^{08}	612813240.642324	620570370.270707
5.1×10^{09}	7148466452.092707	7238953369.207805
5.1×10^{10}	81696759452.488068	82730895648.089188
5.1×10^{11}	918826022119.885010	930456731260.643188
5.1×10^{12}	10212094931561.009766	10341361956011.148438

Table 22. The values of P_D and $P_{D'}$ when $x_{eD} = 2.0000$

t_D	P_D	$P_{D'}$
5.1×10^{03}	1134.563747	1148.925313
5.1×10^{04}	22691.274938	22978.506266
5.1×10^{05}	340344.813725	344652.975924
5.1×10^{06}	4538254.987586	4595701.253251
5.1×10^{07}	56728187.344821	57446265.665642
5.1×10^{08}	680835510.353622	689453681.370756
5.1×10^{09}	7941946228.274997	8042477193.189871
5.1×10^{10}	90765099751.714249	91914025065.027084
5.1×10^{11}	1020815710575.192261	1033737428430.574585
5.1×10^{12}	11345637468964.281250	11489253133128.386719

Acknowledgements

First I thank Allah the Almighty for granting me the strength and insight to peacefully complete this article. My sincere gratitude to my supervisors Dr. Phineas Roy Kiogora and Dr. Kennedy Otieno Awuor for their advice and valuable guidance.
My special thanks goes to African Union for giving me the opportunity to fulfill my dream of pursuing a Master's degree. My appreciation goes to all my lecturers at PAUSTI for the knowledge impacted on me. Finally my profound gratitude to uncle Sulayman Darboe(Mano), uncle Lamin Darboe, uncle Ensa Touray, My lovely wife Mariama Ceesay, and Salifu Demba for their continuous support and encouragement.

References

[1] H. Aghar, M. Carie, H. Elshahawi, J. R. Gomez, J. Saeedi, C. Young, B. Pinguet, K. Swainson, E. Takla, and B. Theuveny, in *Oilfield Review* (2007), vol. 19, pp. 44–59.
[2] C. Temizel, M. Irani, S. Ghannadi, C. H. Canbaz, R. Moreno, F. Bashtani, and M. A. Basri, in *SPE Annual Technical Conference and Exhibition* (OnePetro, 2019).
[3] D. Bourdet, *Well test analysis: the use of advanced interpretation models* (Elsevier, 2002).
[4] A. C. Gringarten and H. J. Ramey, Society of Petroleum Engineers Journal **13**, 285 (1973).
[5] I. Kutasov, L. Eppelbaum, and M. Kagan, Journal of Geophysics and Engineering **5**, 86 (2008).
[6] M. O. Sanni and A. C. Gringarten, in *SPE annual technical conference and exhibition* (OnePetro, 2008).
[7] I. Eiroboyi and P. Obeta, in *Advanced Materials Research* (Trans Tech Publ, 2014), vol. 1025, pp. 974–978.
[8] S. Akin, in *Proceedings of the World Geothermal Congress, Melbourne, Australia* (2015), pp. 19–25.
[9] S. Igba, L. Akanji, and T. Onwuliri, Journal of Oil, Gas and Petrochemical Sciences (2019).
[10] A. Ogbamikhumi and E. Adewole, Nigerian Journal of Technology **39**, 148 (2020).
[11] W. Ouyang, H. Sun, and H. Han, Natural Gas Industry B **7**, 514 (2020).
[12] J. Orene and E. Adewole, Nigerian journal of Technology **39**, 154 (2020).
[13] E. Idudje and E. Adewole, Nigerian Journal of Technology **39**, 816 (2020).
[14] Y.-G. Duan, K.-Y. Ren, Q.-T. Fang, M.-Q. Wei, M. Dejam, and W.-H. Chen, Mathematical Problems in Engineering **2020** (2020).
[15] J. Zhang, S. Cheng, S. Di, Z. Gao, R. Yang, and P. Cao, Geofluids **2021** (2021).
[16] I. Mohammed, T. O. Olayiwola, M. Alkathim, A. A. Awotunde, and S. F. Alafnan, Petroleum Science **18**, 154 (2021).
[17] T. K. Nzomo, S. E. Adewole, K. O. Awuor, and D. O. Oyoo, Open Engineering **12**, 17 (2022).